TITLE: KrF--LASER ANNEALING OF NATIVE OXIDES ON GaAs

AUTHOR(S): R. K. Ahrenkiel, G. Anderson, D. Dunlavy,
C. Maggiore, R. B. Hammond, S. Stotlar

MASTER

los alamos
scientific laboratory
of the University of California
LOS ALAMOS, NEW MEXICO 87544

An Affirmative Action/Equal Opportunity Employer

of laser energy in oxides of 1000 to 2000 Å thickness. Experimentally, laser fluxes greater than 60 mJ/cm^2 produced color changes in the oxide, indicating a change in oxide thickness and/or index of refraction.

Calculations of the energy density deposited in the oxide as a function of distance from the front surface are shown in Fig. 1 for a 2000 Å oxide. Here the input laser flux Φ_0 is a parameter, and the reflection from the interface is
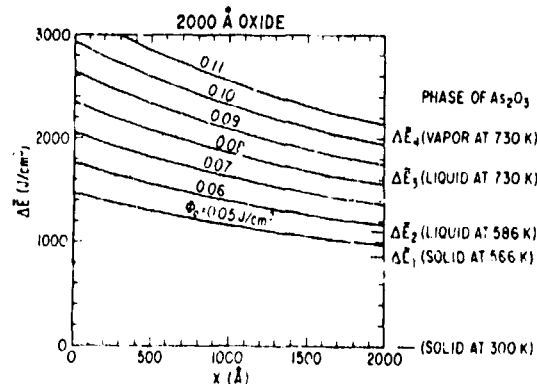

Fig. 1. The calculated energy density in a 2000 Å thick oxide for various laser fluxes.

incorporated in the calculations. The horizontal dotted line represents phase changes in the As$_2$O$_3$ component of the oxide corresponding to the appropriate energy density. A linear model (constant oxide composition as a function of laser flux) was assumed throughout. The model verifies the onset of color change at 50-60 mJ/cm^2 corresponding to the melting of As$_2$O$_3$. These initial color changes are probably related to densification of the somewhat porous as-grown oxide.

Vaporization of As$_2$O$_3$ should occur at fluxes greater than about 110 mJ/cm^2. Our work has shown that evaporation of the As$_2$O$_3$ component occurs at fluxes from 200 mJ/cm^2 to 1.0 J/cm^2.

The "crater" produced by laser annealing has been examined by several techniques. A micro-ellipsometer was used to obtain the data of Fig. 2. Here a focused HeNe laser beam was polarization modulated, and the technique of Jasperson et al. was used to determine the ellipsometric parameters ψ and Δ. From these parameters, the index of refraction n and the oxide thickness t could be determined. A profile of the crater is shown in Fig. 2. Here the oxide thickness has been reduced by about 34% by a 1-J/cm^2 laser pulse. The roughness is believed to be produced by intensity structure in the laser beam. The Los Alamos Scientific Laboratory (LASL) ion microprobe (9) using 5-MeV deuterons produced the oxygen concentration data of Fig. 3. The nuclear reaction $d + {}^{16}O \rightarrow p + {}^*O^{17}$ was used to obtain quantitative oxygen data. The oxygen content here is about 60% of the initial value and scales with the thickness shown in Fig. 2. The primary oxygen loss mechanism

of laser energy in oxides of 1000 to 2000 Å thickness. Experimentally, laser fluxes greater than 60 mJ/cm^2 produced color changes in the oxide, indicating a change in oxide thickness and/or index of refraction.

Calculations of the energy density deposited in the oxide as a function of distance from the front surface are shown in Fig. 1 for a 2000 Å oxide. Here the input laser flux ϕ_0 is a parameter, and the reflection from the interface is
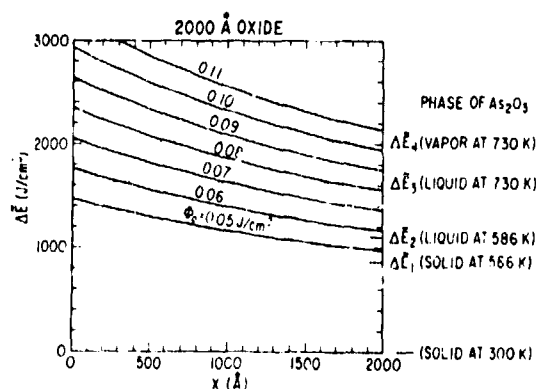

Fig. 1. The calculated energy density in a 2000 Å thick oxide for various laser fluxes.

incorporated in the calculations. The horizontal dotted line represents phase changes in the As_2O_3 component of the oxide corresponding to the appropriate energy density. A linear model (constant oxide composition as a function of laser flux) was assumed throughout. The model verifies the onset of color change at 50-60 mJ/cm^2 corresponding to the melting of As_2O_3. These initial color changes are probably related to densification of the somewhat porous as-grown oxide.

Vaporization of As_2O_3 should occur at fluxes greater than about 110 mJ/cm^2. Our work has shown that evaporation of the As_2O_3 component occurs at fluxes from 200 mJ/cm^2 to 1.0 J/cm^2.

The "crater" produced by laser annealing has been examined by several techniques. A micro-ellipsometer was used to obtain the data of Fig. 2. Here a focused HeNe laser beam was polarization modulated, and the technique of Jasperson et al. was used to determine the ellipsometric parameters ψ and Δ. From these parameters, the index of refraction n and the oxide thickness t could be determined. A profile of the crater is shown in Fig. 2. Here the oxide thickness has been reduced by about 34% by a 1-J/cm^2 laser pulse. The roughness is believed to be produced by intensity structure in the laser beam. The Los Alamos Scientific Laboratory (LASL) ion microprobe (9) using 5-MeV deuterons produced the oxygen concentration data of Fig. 3. The nuclear reaction $d + {}^{16}O \rightarrow p + {}^{*}O^{17}$ was used to obtain quantitative oxygen data. The oxygen content here is about 60% of the initial value and scales with the thickness shown in Fig. 2. The primary oxygen loss mechanism

is probably the vaporization of As_2O_3 as predicted by our calculations. The relative thickness of annealed and unannealed areas was also verified by the deposition of 20-mil diameter gates followed by the measurement of oxide capacit^nce. As shown in Fig. 2, the oxide thickness as determined from $\epsilon A/d_{OX}$ is also about 66% of the initial value. Here A is the cross sectional area and d_{OX} is the oxide thickness.
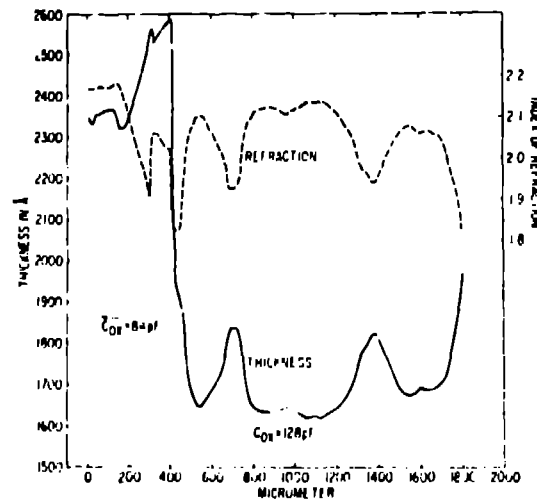

Fig. 2. The thickness and index of refraction of a laser-annealed "crater" with an input flux q_0 of about 1.0 J/cm^2.
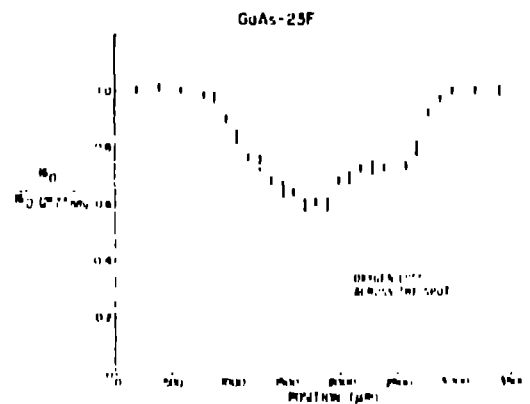

Fig. 3.. The oxygen concentration across the laser-annea'ed crater of Fig. 2 as determined by ion backscattering.

G-V studies of MOS structures both inside and outside the crater show no significant difference in interface properties even though the local temperature may have exceeded 450°C during laser annealing. By comparison, thermal annealing of oxides

at 400°C produces significant interface damage as seen by enhanced G-V loss peaks. Hence laser annealing of oxides appears to be a means of processing native oxides without damaging the interface of the III-V material.

Pulsed 1-MHz capacitance measurements were used to evaluate the slow trap density. Here the MOS structure was pulsed to -20 V for about 10 ms. At the termination of the voltage pulse, the capacitance is given by:

$$C(t) = \frac{C_{OX}}{\sqrt{1-K(V_{FB} + \Delta V_{FB})}} \tag{1}$$

$$\text{where } K = \frac{2C_{OX}^2}{N_A \epsilon A^2} \tag{2}$$

Here ϵ is the oxide dielectric constant, A is the area of the MOS structure, C_{OX} is the oxide capacitance, and N_A is the density of free holes.

The pulsed capacitance recovery is shown in Fig. 4 for three different oxides. Curve A is the recovery of an as-grown oxide. Curve B is the response of a furnace-annealed oxide for an annealing temperature of 350°C--the maximum permissible steady-state temperature that avoids arsenic loss. Curve C results from an oxide that was thermally annealed at 350°C and laser annealed at a flux of 230 mJ/cm².
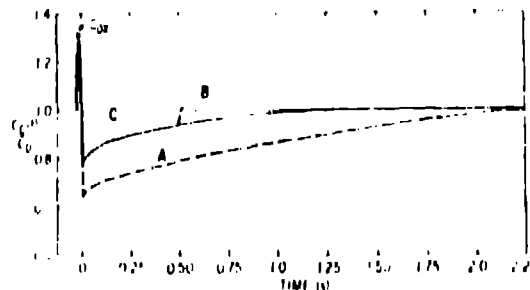

Fig. 4. Pulsed-capacitance recovery for three oxides. A) unannealed; B) thermal-annealed at 350 C; C) thermal-annealed at 350°C plus laser-annealed at 230 mJ/cm².

The charge in oxide traps is:

$$N_{OX}(t) = \frac{C_{OX} |V_{FB}|}{A\epsilon} \tag{3}$$

From the pulsed capacitance recovery, N_{OX} may be calculated as a function of time. Figure 5 shows N_{OX} for the three MOS structures. The reduction of slow oxide

traps with the various treatments is obvious here. Multiple laser pulses seem to produce more desirable changes in the oxide without producing radiation damage. Such studies are still in progress.
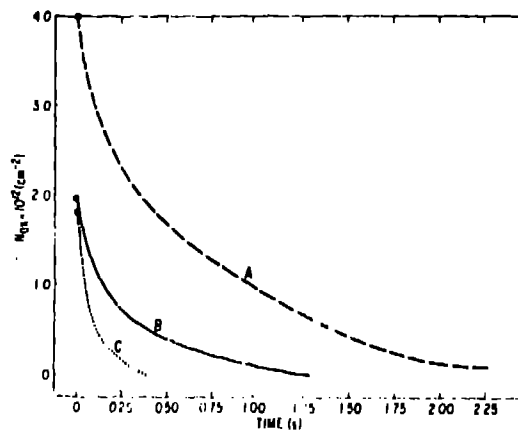

Fig. 5. Concentration of trapped oxide charge for the
three sample of Fig. 4.

Initial studies have shown that the chemical etch rates for laser-annealed areas are different than for unannealed areas. This eff t could be useful in developing new photolithographic processes.

In conclusion, we have demonstrated a new method of changing the physical, chemical, and electronic properties of native oxides grown on GaAs. This method suggests a variety of uses in semiconductor technology.

REFERENCES

(1) For a review see, A. E. Bell, RCA Review 40, 295 (1979).

(2) S. P. Murarka, Appl. Phys. Lett. 26, 180 (1975).

(3) R. P. H. Chang and J. J. Coleman, Appl. Phys. Lett. 32, 332 (1978).

(4) H. Hasegawa, K. E. Frrward, H. L. Hartnagel, Appl. Phys. Lett. 26, 567 (1975).

(5) E. Kohn and H. L. Hartnagel, Solid-State Electron 21, 409 (1978).

(6) C. N. Nicollien and A. Goetzberger, Appl. Phys. Lett. 7, 216 (1965).

(7) E. D. Palik, N. Ginsburg, R. T. Holm, and J. W. Gibson, J. Vac. Sci. Technol. 15, 1488, (1978).

(8) S. N. Jasperson, D. K. Burge, and R. C. O'Handley, Surface Science 37, 548 (1973).

(9) C. M. Maggiore, (to be published) Scanning Electron Microscopy/1980 , edited by Om Johari.